

TOTAL AND EXTREME PRECIPITATION CHANGES OVER THE NORTHEASTERN UNITED STATES

Huanping Huang
Department of Earth Sciences
Dartmouth College
Hanover, NH 03755,

Jonathan M. Winter
Department of Geography
Department of Earth Sciences
Dartmouth College
Hanover, NH 03755,

Erich C. Osterberg
Department of Earth Sciences
Dartmouth College
Hanover, NH 03755,

Radley M. Horton
Columbia University
NASA Goddard Institute for Space Studies
New York, NY 10025,

and

Brian Beckage
Department of Plant Biology
University of Vermont
Burlington, VT 05405

Corresponding Author:
Huanping Huang
6015 Fairchild Hall, Hanover, NH 03755
Huanping.Huang.GR@Dartmouth.edu

Abstract

The Northeastern United States has experienced a large increase in precipitation over recent decades. Annual and seasonal changes of total and extreme precipitation from station observations in the Northeast are assessed over multiple time periods spanning 1901–2014. Spatially averaged, both annual total and extreme precipitation across the Northeast have increased significantly since 1901, with changepoints occurring in 2002 and 1996, respectively. Annual extreme precipitation has experienced a larger increase than total precipitation; extreme precipitation from 1996–2014 was 53% higher than from 1901–1995. Spatially, coastal areas received more total and extreme precipitation on average, but increases across the changepoints are distributed fairly uniformly across the domain. Increases in annual total precipitation across the 2002 changepoint have been driven by significant total precipitation increases in fall and summer, while increases in annual extreme precipitation across the 1996 changepoint have been driven by significant extreme precipitation increases in fall and spring. The ability of gridded observed and reanalysis precipitation data to reproduce station observations was also evaluated. Gridded observations perform well in reproducing averages and trends of annual and seasonal total precipitation, but extreme precipitation trends show significantly different spatial and domain-averaged trends than station data. North American Regional Reanalysis generally underestimates annual and seasonal total and extreme precipitation means and trends relative to station observations, and also shows substantial differences in the spatial pattern of total and extreme precipitation trends within the Northeast.

1 Introduction

Multiple studies have found increasing total and extreme precipitation across the Northeastern United States (Kunkel et al. 2013a; Peterson et al. 2013; Hayhoe et al. 2007), and extreme precipitation events have increased faster over the Northeast region than in any other part of the United States (Kunkel et al. 2013a). Hayhoe et al. (2007) found an increase of 10 mm decade⁻¹ in annual total precipitation from 1900 to 1999 using the 93 stations in the U.S. Historical Climatology Network in the states of Maine, New Hampshire, Vermont, Massachusetts, Rhode Island, Connecticut, New York, New Jersey, and Pennsylvania. Using the U.S. Climate Divisional Dataset Version 2 over the domain of Hayhoe et al. (2007) plus Maryland, Delaware, West Virginia, and Washington D.C., Kunkel et al. (2013b) found a 10.2 mm decade⁻¹ increase in annual total precipitation over 1895–2011. However, across a similar time period (1901–2000) as Hayhoe et al. (2007), Walsh et al. (2014) and Kunkel et al. (2013b) found a trend of approximately 5.6 mm decade⁻¹.

Extreme precipitation events have also been increasing across the Northeast, both in intensity and frequency, particularly over the past three decades (Walsh et al. 2014; Kunkel et al. 2013a; Hoerling et al. 2016). This increase in extreme precipitation events is consistent with expected impacts of climate change on precipitation, primarily more extreme events driven by the ability of the atmosphere to hold more water as described by the Clausius-Clapeyron relationship (e.g., Trenberth 1998; Mishra et al. 2012; Prein et al. 2017). Kunkel et al. (2013a) found significant increases in both 1-in-5-year 2-day precipitation events and the amount of precipitation falling on the 1% wettest days during the time period 1957–2010 for the Northeast. Hoerling et al. (2016) discovered a 2–3% increase per decade in both the total amount and frequency of heavy precipitation events (5% wettest days) in the Northeast over 1901–2013, with the increases in

heavy precipitation total amount, frequency, and intensity accelerating after 1979. Walsh et al. (2014) also evaluated trends in the amount of precipitation falling in the Northeast on the 1% wettest days using the Global Historical Climatology Network-Daily dataset, finding a striking increase of 71% from 1958 to 2012.

Given the growing consensus on the recent dramatic increase of extreme precipitation across the Northeast, our motivation is to explore the temporal and spatial attributes of precipitation increases in greater detail, as well as assess the ability of gridded observational and reanalysis datasets to capture this precipitation increase. Specifically, we add to this literature by: 1. assessing the sensitivity of total and extreme precipitation changes to the time period of analysis (Sections 3.1.1, 3.1.3), 2. exploring the spatial distribution of total and extreme precipitation across the Northeast (Sections 3.1.2, 3.1.4), 3. analyzing seasonal contributions to changes in annual total and extreme precipitation (Sections 3.1.5), and 4. evaluating the consistency of means and trends in precipitation across station, gridded, and reanalysis data (Section 3.2).

2 Data and Methods

We define the Northeast as Maine, New Hampshire, Vermont, Massachusetts, Connecticut, Rhode Island, New Jersey, New York, Pennsylvania, Maryland, Washington D.C., Delaware, and West Virginia. This domain was selected for consistency with Walsh et al. (2014). This study focuses on precipitation changes recorded by station observations since 1901, which are variable in length by station, as well as gridded and reanalysis data spanning 1915–2011 and 1979–2014, respectively. We therefore conduct our analyses for three time periods: 1901–2014, 1915–2011, 1979–2014. To facilitate intercomparisons among the three datasets, an additional

period, 1979–2011, is also analyzed. Each of the three datasets used – station observations, gridded observations, and reanalysis – as well as the metrics and processes used to analyze them, are described below.

2.1 Climate Data

Station observations were derived from the Global Historical Climatology Network-Daily (GHCN-D) dataset (Menne et al. 2012a, b), which is produced and archived by the National Oceanic and Atmospheric Association (NOAA) National Climatic Data Center. GHCN-D has been used extensively in climate analysis and monitoring studies that require daily data, such as assessments of heavy rainfall events, heat waves and cold snaps, and is the official archive for US daily data (Menne et al. 2012b; Peterson et al. 2013). It consists of over 96,000 stations worldwide that capture all or a subset of: daily maximum and minimum temperature, precipitation, snowfall, and snow depth. The time period of record varies by station from less than one year to 177 years, with the average precipitation record spanning 33.1 years (Menne et al. 2012b).

Because the temporal coverage of GHCN-D varies, we first extracted all 5,867 stations for the Northeast domain as defined above and then selected stations based on an 80% completeness threshold (Alexander et al. 2006; Xie et al. 2007; Higgins et al. 2007). We first require that each year be at least 80% complete and treated years with less than 80% complete records as missing values in order to minimize the potential influence of years with seasonal gaps. Then, we selected stations with daily records at least 80% complete in one or two periods (1901–2014:

80% complete overall and 80% complete from 1979–2014; 1915–2011: 80% complete from 1915–2011 and 80% complete from 1979–2011; 1979–2014: 80% complete from 1979–2014; 1979–2011: 80% complete from 1979–2011). Applying these standards yields 116 qualifying stations for the 1901–2014 period, 176 stations for the 1915–2011 period, 558 stations for the 1979–2011 period, and 525 stations for the 1979–2014 period. To calculate annual total precipitation, daily precipitation amounts were averaged and then multiplied by the total days of each year.

Gridded observations were developed by Livneh et al. (2013), hereafter LI2013, for the contiguous United States based on the methods of Maurer et al. (2002). Maurer et al. (2002) has been widely used in water and energy budget studies as well as climate change assessments (Wood et al. 2004; Hayhoe et al. 2004; Westerling et al. 2006; Elsner et al. 2014). LI2013 uses daily temperature and precipitation observations from approximately 20,000 NOAA Cooperative Observer (COOP) stations gridded to a spatial resolution of $1/16^\circ$ latitude/longitude (~ 7 km). Available daily meteorological data include station-based temperature and precipitation, as well as wind from reanalysis covering the time period 1915–2011 (Livneh et al. 2013). Additional details of LI2013 can be found in Livneh et al. (2013) and Maurer et al. (2002).

Reanalysis data are from the National Centers for Environmental Prediction (NCEP) North American Regional Reanalysis (NARR; Mesinger et al. 2006). NARR combines NCEP's Eta atmospheric model and Regional Data Assimilation System to produce a dynamically consistent atmospheric and land surface hydrology dataset for North America (Mesinger et al. 2006). Compared to other reanalysis products, NARR is high resolution (~ 32 km) and notably

incorporates precipitation, a variable not typically assimilated (Mesinger et al. 2006). Further, NARR uses an updated version of the NOAA land surface model and an expanded and improved set of observations for data assimilation (Mesinger et al. 2006). NARR has been shown to have significantly improved performance relative to NCEP-Department of Energy Reanalysis 2 (Mesinger et al. 2006). NARR is available at 3-hour, daily and monthly temporal resolutions for 1979 to near present; we use daily means from 1979–2014. To make NARR directly comparable to gridded observations, we interpolated its native Lambert Conformal Conic grid to $1/16^\circ$ regular latitude using the nearest neighbor approach of MATLAB's griddata function.

2.2 Methods

Using the three datasets described above, we assess annual and seasonal changes in total and extreme precipitation over the Northeast spanning multiple time periods, both spatially averaged and at the station/grid scale. Time periods are selected to maximize overlap across datasets and for consistency with Walsh et al. (2014). Analyses were conducted for each dataset – GHCN-D, NARR, and LI2013 – individually, and then the consistency of changes across datasets was evaluated.

Stations with long-term records are distributed unevenly in the Northeast with a higher station density near major and largely near-coastal metropolitan areas and a lower density in mountainous regions. To properly represent the regional values from station observations, we applied area averaging to calculate regional precipitation means (Groisman et al. 2004) instead of simply averaging over all stations. Area averaging is conducted by arithmetically averaging annual or seasonal precipitation values in all stations within $1^\circ \times 1^\circ$ grid cells and then regionally

averaging the gridded values (Groisman et al. 2004; Walsh et al. 2014). Grid cells without any selected GHCN-D stations are treated as missing values, and therefore do not get incorporated in the regional means.

We calculate annual total precipitation by calendar year for all three daily datasets over the length of record, as well as for a few select time periods described in Section 2.1 to enable comparisons across datasets. Then, for each data point within the domain (station for station observations, grid cell for gridded observations and NARR), we calculate a linear regression from the annually averaged values, yielding an annual trend for all relevant time periods. Simple linear regression is used as the standard parametric trend analysis method with a significance test (Student's t-test) at $p < 0.05$. To make the trends in precipitation (absolute changes, expressed in mm decade^{-1}) more comparable among various periods, we also compute relative percent changes (expressed in $\% \text{ decade}^{-1}$) by subtracting the first point on the linear regression from the last point on the regression, and then dividing by the modeled value at the first point:

$$\Delta = \frac{10 * S}{P_i} * 100\% \quad (1)$$

where Δ is the relative change in precipitation ($\% \text{ decade}^{-1}$), S is the slope of the linear model (mm yr^{-1}), and P_i is the modeled precipitation value in start year i (mm). In addition to assessing linear trends in total precipitation with Student's t-test, we also conducted a rank-based Mann-Kendall significance test for annual total precipitation.

In the seasonal precipitation analyses, daily records were grouped into four seasons: spring (March, April, May), summer (June, July, August), fall (September, October, November), and winter (December, January, February). For station observations, seasonal total precipitation in each year was calculated by multiplying the daily average in a season by the total days of the season, consistent with the calculation of annual total precipitation. Because the selected stations are constrained by the 80% complete requirement in both total daily records and annual records, seasonal records were usually at least 60% complete (higher than 80% complete in most seasons). For gridded and reanalysis data, seasonal total precipitation is the sum of daily precipitation amounts in a season because both datasets provide complete daily values. The winter seasonal time series contains one less value than other seasonal series because January and February in both 2012 and 2015 fall outside the analysis periods ending in 2011 and 2014, respectively. Seasonal trends and changes in total precipitation were calculated with the same methods as annual total precipitation.

We define extreme precipitation as the amount of precipitation falling on the 1% of wet days recording the most precipitation. Specifically, for each station (for GHCN-D) or grid cell (for LI2013 and NARR), we first determined the 99th percentile threshold of daily precipitation events over each of the four periods of record (1901–2014, 1915–2011, 1979–2014, and 1979–2011). Then, for each station or grid point, we summed the total precipitation falling on days exceeding the 99th percentile threshold for each year. These annual values were then averaged by area for stations (or by grid cells for gridded observations and reanalysis) to determine the Northeast regional annual values of extreme precipitation. This procedure is consistent with Walsh et al. (2014). We repeated this process by season to calculate seasonal extreme

precipitation values using 32 thresholds in total for the three datasets, four periods, and four seasons. It is important to note that we calculate different 99th percentile extreme precipitation thresholds for each season. For example, the average Northeast thresholds are 38.9 mm in winter vs. 55.1 mm in summer from 1901–2014 in the GHCN-D dataset. Thus, the seasonal extreme precipitation means may appear to suggest relatively equal amounts of extreme precipitation in each season, whereas at least 75% of the 99th percentile events in the Northeast occur in summer and fall when using a single extreme threshold for the whole year (Frei et al. 2015). Thus, applying the same threshold to each season would result in small or negligible amounts of winter and spring extreme precipitation, making comparisons of gridded and reanalysis precipitation to station observations very difficult.

Trends in annual and seasonal extreme precipitation were assessed using a non-parametric, Theil-Sen robust linear regression (Theil 1950; Sen 1968). Compared to the parametric trend analysis, i.e. simple linear regression used for total precipitation, the advantages of Theil-Sen estimation is its insensitivity to outliers, making it more accurate than simple linear regression for skewed and heteroskedastic data with multiple extreme values (Alexander et al. 2006; Kunkel et al. 2010). The significance of monotonic trends ($p < 0.05$) from Theil-Sen estimation is evaluated using the Mann-Kendall test (Mann 1945; Kendall 1970). After computing the trends of absolute changes (mm decade^{-1}), relative changes in extreme precipitation ($\% \text{ decade}^{-1}$) are also calculated with equation (1).

We note that in Section 3.1 and Tables 1–4 we use the 116 GHCN-D stations with 80% complete records from 1901–2014 and a single threshold for each station 1901–2014 to determine the 1% extreme precipitation events, which allows us to compare total and extreme precipitation amounts across four time periods. However, we use all GHCN-D stations with 80% complete records (525 stations 1979–2014, 558 stations 1979–2011, 176 stations 1915–2011) for comparison to NARR and LI2013 in Section 3.2 and Tables 5–8.

3 Results and Discussion

We first explore the changes in total and extreme precipitation over the length of record using station observations. Specifically, we analyze annual total and extreme precipitation and their trends (in both absolute and relative changes) across various time periods, and evaluate their spatial distributions. Seasonal total and extreme precipitation are then assessed in a similar way. Finally, we evaluate total and extreme precipitation and their seasonality in gridded observations and reanalysis data, and compare them to the station observations.

3.1 Total and extreme precipitation in station observations

3.1.1 Spatially averaged changes in Northeast total precipitation

GHCN-D annual total precipitation averaged over the Northeast region increased significantly ($p < 0.05$) across all four time periods analyzed using linear regression with a Student’s t-test and for 1979–2011 and 1979–2014 using the Mann-Kendall test (Table 1). The annual total precipitation over both 1979–2014 (1104 mm) and 1979–2011 (1104 mm) was 4.4% higher than the 1901–2014 average (1063 mm). Further, these two recent periods show much larger

increasing trends of 40.8 mm decade⁻¹ (4.0% decade⁻¹) and 52.8 mm decade⁻¹ (5.2% decade⁻¹), respectively, compared to trends over 1901–2014 (6.0 mm decade⁻¹) and 1915–2011 (11.1 mm decade⁻¹) (Table 1). In fact, linear trends ending in 2014 consistently increase in slope as the start date progressively moves through the 20th century (Figure 1a), confirming that linear trends in annual total precipitation in the Northeast are highly sensitive to both the start and end dates as noted in other precipitation analyses (Frei et al. 2015; Frei and Schär 2001; Wu et al. 2005).

Interestingly, when starting from 1901, the linear trend does not become significant until 2014, and the trend from 1901–2001 is -1.6 mm decade⁻¹. Kunkel et al. (2013b) note a significant increase in total Northeast precipitation from 1901–2011, but an analysis of their data shows that there is no significant trend from 1901–2001, similar to our findings. We conclude that the shift to a wetter climate in 2002 (Figure 1b) is responsible for the significant linear trends in annual total precipitation from 1901–2014 and the progressively larger trends in recent decades (Figure 1a).

A changepoint analysis using the findchangepts function in MATLAB (Killick et al. 2012) identifies the abrupt shift to a wetter period in 2002 (Figure 1b). Every annual total from 2002 to 2014 was above the 1901–2014 average (1063 mm), which never occurred in any previous 13-yr period. Total precipitation increased by 13% across this changepoint, with a mean from 1901–2001 of 1048 mm and from 2002–2014 of 1183 mm. There are insignificant decreasing trends both before the 2002 shift (-1.6 mm decade⁻¹ from 1901–2001) and after (-62.9 mm decade⁻¹ from 2002–2014), indicating that a changepoint analysis is preferable to a linear trend analysis to characterize the change in total precipitation from 1901–2014. Future analyses will focus on

identifying the dynamical changes underlying this abrupt increase in Northeast precipitation around 2001–2002.

We attribute differences between the trends calculated in Kunkel et al. (2013b), Hayhoe et al. (2007), and this work to differences in datasets analyzed, spatial domain, data processing and quality control procedures (e.g. filling missing daily data and the spatial gridding method), and bias correction due to historical changes in instrumentation and observing practices (Legates and DeLiberty 1993; Vose et al. 2014; Menne et al. 2012a, b; Easterling et al. 1996).

3.1.2 Spatial changes in Northeast total precipitation

Shifting our focus to the spatial patterns of precipitation rates and trends over the Northeast (Figure 2), we find the expected coast-interior gradient with coastal areas generally receiving more annual total precipitation, although some mountainous stations in northern West Virginia and central New York also received very high precipitation ($>1200 \text{ mm yr}^{-1}$) due to orographic effects (Kunkel et al. 2013b). Despite the substantial coast-interior gradient in total precipitation amount, total precipitation trends from 1901–2014 and 1915–2011 were generally consistently positive across the whole Northeast domain, with the exception of decreases or no significant trends in parts of West Virginia, eastern Maryland and Delaware (Figure 2b, 2c). Fifty-five of the 116 stations (47%) had statistically significant positive trends from 1901–2014, whereas only 17 stations (15%) from 1901–2014 had negative annual total precipitation trends, and only three of these (all in West Virginia) were statistically significant (Figure 2b). Similarly, 49% and 2% of stations experienced significant increasing and decreasing trends from 1915–2011, respectively. Relative to the longer-term period of 1901–2014, the 1979–2014 interval features a higher

proportion (90%) of stations with positive trends, with only 10% of the stations showing negative trends (Figure 2d). However, only 26% of the stations show positive trends that are statistically significant, although they are distributed relatively uniformly across the Northeast domain similar to the 1901–2014 trend pattern.

3.1.3 Spatially averaged changes in Northeast extreme precipitation

Recent increases in extreme precipitation over the Northeast are significantly larger than the increases in annual total precipitation described above. Annual extreme precipitation averaged 82.4 mm yr⁻¹ from 1901–2014, and increased significantly by 2.4 mm decade⁻¹ (3.6% decade⁻¹) over this interval (Table 2). The positive trends in extreme precipitation ending in 2014 progressively increase with later start years (Figure 3a), in parallel with the total precipitation trends. These large trends in extreme precipitation are dominated by high annual extremes since 1996 (Figure 3), with the four highest extreme precipitation years in 2011 (182.8 mm), 1996 (177.3 mm), 2005 (177.2 mm), and 2010 (157.9 mm). From 1996 to 2014, all but two annual extremes (1997 and 2001) are above the 1901–2014 average (Figure 3b). Similar to annual total precipitation, there is no significant trend in extreme precipitation from 1901–1995. Thus, long-term trends in extreme precipitation are likewise very sensitive to the length of records, start year, and end year.

As with total precipitation changes, changes in extreme precipitation from 1901–2014 are not well characterized by a linear trend. The changepoint algorithm identifies the 1996 jump to higher extreme precipitation that is apparent visually in the time series (Figure 3b). Averaged

over the Northeast, extreme precipitation from 1996–2014 was 53% higher than from 1901–1995. Interestingly, there is no significant trend within the wetter 1996–2014 interval, although the 19-year length is too short to assess trends with confidence.

Walsh et al. (2014) reported a striking extreme precipitation increase in the Northeast of 71% from 1958 to 2012, which exceeds all other regions in the continental U.S. Following the same calculation procedures as Walsh et al. (2014), we find a comparable increase (69%) in extreme precipitation relative to the 1958–2012 average. However, extreme precipitation increased only by 8.4% over the period 1958–1995, and the trend is insignificant. Therefore, we argue that the 53% increase in average extreme precipitation after the 1996 changepoint is more representative of the increase in Northeast extreme precipitation.

3.1.4 Spatial changes in extreme precipitation

Figure 4a shows that, as expected, coastal areas generally received more extreme precipitation than inland areas from 1901 to 2014, which mirrors the spatial pattern in annual total precipitation. Also as in annual total precipitation, there is a pocket of elevated extreme precipitation driven by topography in northern West Virginia.

In terms of spatial patterns in the extreme precipitation trends, annual extreme precipitation increased in 58 (50%) of the 116 stations from 1901 to 2014 (Figure 4b), 30 (25%) of which were statistically significant. The stations with positive extreme precipitation trends are distributed fairly uniformly throughout the study area (Figure 4b). Only five (4.3%) stations had

negative trends, two of which were significant. The remaining 53 stations (45.7%) had an undetectable trend because more than half of the annual values for those stations were zero, and the Theil-Sen estimator calculates the median slope of all possible lines between any two paired points (Theil 1950; Sen 1968). This large proportion of zeroes in the station extreme precipitation time series is a result of heavy precipitation events occurring over limited time period relative to the length of record, which limits our ability to assess trend significance by station. However, this limitation does not affect the trend values themselves or the detection of spatially averaged trends as described in Section 3.1.3.

The more recent period of 1979–2014 contains a higher proportion of stations with positive trends (315 out of 525 stations, or 60%), 79 (15%) of which are statistically significant (Figure 4d). Once again, the stations showing positive trends are distributed throughout the study area, with the exception of western New York State and Pennsylvania (Figure 4d) where several of the 40 stations (7.6%) with decreasing trends are located. Only 3 stations (0.6%) have statistically significant decreases in extreme precipitation: Bradford Regional Airport, Pennsylvania (41.80° N, 78.64° W), Erie International Airport, Pennsylvania (42.08° N, 80.18° W), and Ashfield, Massachusetts (42.51° N, 72.85° W). Bradford and Ashfield are two of the three stations that have a significant decrease in annual total precipitation as well. Bradford Regional Airport and Erie International Airport are both located just east of Lake Erie in a local area with multiple stations reporting decreases in extreme precipitation, while Ashfield is anomalous based on surrounding stations.

Figure 5 shows the percent difference in extreme precipitation between the wetter 1996–2014 period compared to 1901–1995, representing the change across the 1996 changepoint. 105 of the 116 stations (91%) show higher extreme precipitation after 1996, and 56 stations exceed a 50% increase and are fairly uniformly distributed across the Northeast (Figure 5). Regions with multiple stations showing an extreme precipitation decrease across this changepoint include east of Lake Erie (western New York and Pennsylvania) and northeast West Virginia. Thus, these regions consistently show declining recent trends in total (Figure 2d) and extreme precipitation (Figures 4d and 5).

3.1.5 Changes in seasonal precipitation

Total precipitation increases in spring, summer, and fall over all four time periods of analysis (Table 3), with larger trends since 1979, consistent with the record of increasing annual total precipitation (Table 1). Over the full time period (1901–2014), only the trend in fall precipitation ($4.8 \text{ mm decade}^{-1}$) is significant, while the summer trend ($18.3 \text{ mm decade}^{-1}$) is significant over 1979–2014 (Table 3). These findings are consistent with Kunkel et al. (2013b), who reported fall as the only season that experienced a significant increase in total precipitation 1895–2011, Frei et al. (2015), who found that precipitation during the warm season (June–October) increased after 2002, and Marquardt Collow et al. (2016), who noted a significant increase in mean summer (June, July, August) precipitation over the period 1979–2014. Fall and summer precipitation experience changepoints in 2002 and 2003, respectively, suggesting that these two seasons are important drivers of the annual total precipitation changepoint in 2002. Winter precipitation, in contrast, shows a distinctly different pattern: a decreasing trend ($-1.8 \text{ mm decade}^{-1}$) from 1901–2014, a near-zero trend ($0.6 \text{ mm decade}^{-1}$) from 1915–2011, and large, statistically significant

trends (18.1–21.8 mm decade⁻¹) since 1979. However, the large trends since 1979 are strongly influenced by the winter 1979 value, which is the lowest in the entire record. Extending the period back just two additional years to 1977 (e.g. 1977–2014) results in lower winter trends by a factor of 2–3 that are statistically insignificant (not shown), providing further evidence of the sensitivity of trend analysis to time period analyzed.

Extreme precipitation increases across all seasons over all time periods, with the largest percentage increases in spring and winter. These increases are statistically significant for winter (all periods) and for spring over the long periods (1901–2014 and 1915–2011), as shown in Table 4. Trends are particularly large over 1979–2014 across all seasons, and seasonal contributions to the abrupt annual extreme precipitation shift in 1996 are dominated by increases in spring and fall extreme precipitation, which are 83% and 85% higher from 1996–2014 than from 1901–1995, respectively. Winter and summer extreme precipitation are 45% and 27% higher, respectively, after the 1996 shift (not shown). In addition, fall extreme precipitation contains a changepoint in 1995, one year before the annual extreme precipitation changepoint. The spring extreme precipitation changepoint occurred in 2005, but it moves to 1998 if 2003, one of the 10 lowest extreme springs on record, is removed. Thus, both fall and spring show a significant and abrupt increase in extreme precipitation in the mid-late 1990's that contributed to the annual extreme changepoint in 1996. The similar timing of the fall and spring change to wetter extreme conditions suggests that they may be driven by common dynamical changes.

3.2 Comparison of gridded and reanalysis precipitation to station observations

3.2.1 Spatially averaged Northeast total precipitation

Overall the gridded LI2013 dataset reproduces observed station total precipitation and its trends well. The annual total precipitation during 1915–2011 and 1979–2011 in LI2013 are 1088 and 1143 mm, respectively, compared to 1071 and 1110 mm for the same periods in GHCN-D (Table 5). The 1979–2011 annual precipitation trend in LI2013 ($54.2 \text{ mm decade}^{-1}$) is slightly lower than the trend in GHCN-D ($56.8 \text{ mm decade}^{-1}$), while the trend during 1915–2011 ($12.4 \text{ mm decade}^{-1}$) is slightly higher than the GHCN-D trend ($10.7 \text{ mm decade}^{-1}$). Additionally, consistent with GHCN-D, trends in LI2013 significantly increase from 1915–2011 using linear regression with a Student's t-test and from 1979–2011 using linear regression with a Student's t-test and the Mann-Kendall test. The changepoint algorithm identifies a significant shift to wetter conditions in the LI2013 dataset in 2003, only one year later than the changepoint in the GHCN-D data. Figure 6a shows that LI2013 also closely reproduces the spatial distribution of annual total precipitation observed at GHCN-D stations from 1915–2011. LI2013 also reasonably captures GHCN-D total precipitation trends, although there are differences, such as LI2013 containing a drying trend in western Maine compared to a significant wetting trend in GHCN-D (Figure 6b).

NARR annual total precipitation for 1979–2014 is 1041 mm, compared to 1111 mm in GHCN-D for the same period. With an underestimation of 6.3%, this difference is larger than that found between LI2013 and GHCN-D. In contrast to significant trends in GHCN-D, trends in NARR annual precipitation are insignificant in both periods analyzed (1979–2014 and 1979–2011), and are a remarkable 2–9 times lower than the GHCN-D trends (Table 5). Furthermore, the changepoint analysis identifies no significant changepoints in the NARR annual total

precipitation time series. Spatially, Figure 6c shows that while NARR generally captures the lower annual precipitation values at inland GHCN-D stations, NARR tends to underestimate annual precipitation at other GHCN-D stations. More notable, however, is that NARR has decreasing total precipitation trends in many areas over the period 1979–2014, particularly along the coast and in western Pennsylvania, New York, and West Virginia (Figure 6d). In contrast, GHCN-D has positive trends consistently across most stations in the domain.

We note a few attributes of the source data and development of GHCN-D, LI2013, and NARR that are likely responsible for their disagreement. Although GHCN-D and LI2013 are developed from original observations of COOP stations, LI2013 uses far more stations (about 20,000) with less strict completeness criterion (at least 20 years of valid data) through the contiguous U.S. compared to our 176 GHCN-D stations in the Northeast fulfilling the 80% completeness threshold from 1915–2011 (Livneh et al. 2013; Menne et al. 2012a, b). Precipitation data in the LI2013 dataset is also linearly apportioned among days based on the time of observation to very fine spatial resolution ($1/16^\circ$) and subsequently scaled on a monthly basis so as to match the long-term mean (Livneh et al. 2013), which the authors caution may make the data unsuitable for trend analysis (Livneh et al. 2015). However, we find that despite monthly scaling, LI2013 trends closely match the GHCN-D trends in annual total precipitation.

We note two relevant challenges with NARR. The first is that some discontinuities exist along the U.S.–Canada border (Luo et al. 2007; Milrad et al. 2012). These discontinuities can be attributed to characteristics of the two different national observational datasets, in particular the different spatial density of assimilated rain gauges, merged by NCEP, and the fact that no

smoothing was applied when these two datasets were merged (Mo et al. 2005; Luo et al. 2007; Milrad et al. 2012). To lessen the effects of this discontinuity in our analyses, we masked out a buffer of cells along the U.S.–Canada border. The second challenge is the sharp precipitation gradients along the coastline. Due to lack of station observations, the merged precipitation dataset from the Climate Prediction Center in NCEP is known to be increasingly less reliable over the oceans north of 42.5°N (Mesinger et al. 2006). Thus, NARR is meant to be primarily used over land and may be inaccurate over northern oceans (Mesinger et al. 2006; Bukovsky and Karoly 2007). This provides a likely explanation as to why NARR grids near coastlines, incorporating some information from ocean grid points, have lower precipitation relative to GHCN-D stations.

3.2.2 Spatially averaged Northeast extreme precipitation

LI2013 reproduces the regional average extreme precipitation, but LI2013 extreme precipitation trends differ from the GHCN-D trends (Table 6), contrary to the ability of LI2013 to capture annual total precipitation trends as noted above. Specifically, the trends in extreme precipitation during 1915–2011 and 1979–2011 in LI2013 are lower than GHCN-D, and unlike GHCN-D, they are not statistically significant, nor do they have a statistically significant changepoint. LI2013 reproduces well the GHCN-D spatial pattern of extreme precipitation amount (Figure 7a), but the 1915–2011 LI2013 trends, both positive and negative, are substantially larger over many regions than the GHCN-D trends (Figure 7b).

Like annual total precipitation, NARR also tends to underestimate extreme precipitation (Table 6). The 1979–2011 annual extreme precipitation in NARR (77.5 mm) is 9.9% lower than in GHCN-D (86 mm). While the NARR trend in 1979–2014 annual extreme precipitation (4.9 mm decade⁻¹) is insignificant and much lower than the GHCN-D trend (12.6 mm decade⁻¹), the NARR trend (15.8 mm decade⁻¹) is similar to the GHCN-D trend (14.7 mm decade⁻¹) if the analysis is restricted to 1979–2011. The differences mainly derive from anomalously low extreme precipitation in NARR for 2013–2014; approximately 45% lower than the 1979–2014 average NARR extreme precipitation (77.5 mm). In contrast, the 2013–2014 extreme precipitation in GHCN-D is almost equal to its 1979–2014 average. In further contrast with the GHCN-D data, the NARR extreme precipitation time series has no significant changepoints. Spatially, Figure 7c shows a widespread underestimation of average extreme precipitation by NARR relative to GHCN-D from 1979–2014. NARR does capture GHCN-D trends in extreme precipitation from 1979–2014 in several regions, including central and western New York, western Maine, Delaware, western West Virginia, and southern New Jersey, but otherwise shows significant differences from GHCN-D spatial trends. These spatial differences are largest in New Hampshire, Massachusetts, Vermont, Connecticut and Rhode Island (Figure 7d).

3.2.3 Seasonal precipitation

Relative to GHCN-D, LI2013 slightly overestimates seasonal total precipitation while NARR underestimates seasonal total precipitation (Table 7). Low seasonal total precipitation values in NARR are consistent with the low annual total values in NARR noted in section 3.2.1.

LI2013 seasonal total precipitation trends are similar to GHCN-D trends, whereas trends in NARR are lower than those in GHCN-D. Of the five significant seasonal trends in GHCN-D, two occur during time periods that overlap with LI2013 (1915–2011 fall and 1979–2011 winter), and LI2013 is also significant for both. However, there are three significant trends in GHCN-D for time periods that NARR is available, and NARR matches with 1979–2011 winter only, although it still underestimates the value (15.9 mm decade⁻¹ for NARR compared to 20.1 mm decade⁻¹ for GHCN-D).

For seasonal extreme precipitation (Table 8), once again LI2013 averages are very close to GHCN-D seasonal extreme precipitation averages, whereas NARR generally underestimates seasonal extreme precipitation, with the biggest differences in summer (15%) and smallest differences in winter (0.6%). The seasonal extreme precipitation trends of LI2013 are equal to or smaller than those from GHCN-D, however LI2013 fails to capture most significant seasonal trends in GHCN-D (except winter 1979–2011). NARR seasonal extreme precipitation trends are, similar to seasonal total precipitation trends, equal to or smaller than GHCN-D trends in most cases with the exceptions of spring and fall 1979–2011. Of the four significant positive trends in GHCN-D seasonal extreme precipitation that occur in time periods for which NARR data is available, NARR is significant for two of them, spring and winter 1979–2011.

4 Conclusions

Over the 1901–2014 station observational record in the Northeast, we find a significant 6.8% (0.6% decade⁻¹) increase in annual total precipitation and a much larger 41% (3.6% decade⁻¹) increase in annual extreme precipitation. However, a key conclusion of our study is that the recent increases in annual total and extreme precipitation in the Northeast are best characterized as abrupt shifts in 2002 and 1996, respectively, rather than long-term increases over several decades as could be implied from a linear trend. While the pre-changepoint trends in annual total (1901–2001; -1.6 mm decade⁻¹) and annual extreme (1901–1995; 0.1 mm decade⁻¹) precipitation are not statistically significant, total precipitation from 2002–2014 was 13% higher than from 1901–2001 and extreme precipitation from 1996–2014 was 53% higher than from 1901–1995, with both increases being statistically significant. The fact that these wetter periods both abut the end of our record in 2014 means that any long-term linear trends are highly dependent on their start date, and should therefore be interpreted with caution, particularly when extrapolating into the future. Of note, the recent 2015–2016 drought in the Northeast is not included in our analyses, although it is not likely to change the significance of the post-changepoint increases.

Spatially, we find that the increases in annual total and extreme precipitation are widespread across the Northeast domain, with the exception of smaller increases and even some significant decreases to the east of Lake Erie, and in the southern part of the domain in West Virginia, Maryland, and Delaware. Our seasonal analysis reveals that fall and summer total precipitation have statistically significant increases after changepoints in 2002 and 2003, respectively, suggesting that they contribute to the annual total precipitation changepoint in 2002. The extreme precipitation increase across the 1996 changepoint is associated with 83% and 85% increases in

spring and fall extreme precipitation, respectively, and may indicate common atmospheric forcing of spring and fall extreme precipitation in the mid-late 1990's. The increase in fall precipitation across the 1995 changepoint is consistent with Kunkel et al.'s (2010) finding that increased heavy precipitation associated with tropical cyclones after 1994 is an important driver of the overall increase in extreme precipitation. Our ongoing investigations into the underlying dynamical causes for Northeast annual total and extreme precipitation increases are focusing on these critical time periods in the late 1990s and early 2000s.

Our comparison of spatial and temporal extreme precipitation patterns in station (GHCN-D), gridded (LI2013), and reanalysis (NARR) datasets shows that LI2013 is more consistent with station data than NARR. LI2013 reasonably captures the mean (within 2%) and seasonality (overestimates by 0–10%) of GHCN-D extreme precipitation, but contains significant differences in its trends. NARR underestimates regionally averaged extreme precipitation across all seasons by 0.6–15%, and the annual extreme trends show significant differences in their spatial distribution, particularly over New England. Perhaps more importantly, both the NARR and LI2013 annual extreme time series have no significant changepoints.

LI2013 does, however, reproduce GHCN-D regionally averaged annual and seasonal total precipitation within 5% (and usually within 3%), and its trends faithfully capture those from station observations both across the region and averaged over the Northeast. In addition, LI2013 has a changepoint in 2003, only one year later than the changepoint identified in GHCN-D annual total precipitation. However, NARR underestimates annual and seasonal total precipitation by 3–10%, and has annual total precipitation trends that are a factor of 2–9 times

smaller than GHCN-D trends. Spatially, NARR is also less accurate than LI2013, with decreasing 1979–2014 trends over much of the coastal and western portions of the domain where GHCN-D trends are positive. This comparison of LI2013 and NARR to GHCN-D provides important information on the strengths and limitations of these products for use in analyzing hydroclimate, forcing climate impacts models, and identifying drivers of total and extreme precipitation.

Acknowledgments

Station observation, gridded observation, and reanalysis data are available at <ftp://ftp.ncdc.noaa.gov/pub/data/ghcn/daily/>, <ftp://ftp.hydro.washington.edu/pub/blivneh/CONUS/>, and <http://www.ncdc.noaa.gov/data-access/model-data/model-datasets/north-american-regional-reanalysis-narr>, respectively. We thank our editor and reviewers for their thoughtful feedback. This work was supported by the Vermont Experimental Program for Stimulating Competitive Research (NSF Awards EPS-1101317 and OIA 1556770).

References

- Alexander, L. V., and Coauthors, 2006: Global observed changes in daily climate extremes of temperature and precipitation. *Journal of Geophysical Research: Atmospheres*, **111**, D05109, doi:10.1029/2005JD006290.
- Bukovsky, M. S., and D. J. Karoly, 2007: A Brief Evaluation of Precipitation from the North American Regional Reanalysis. *J. Hydrometeor*, **8**, 837–846, doi:10.1175/JHM595.1.
- Easterling, D. R., T. R. Karl, E. H. Mason, P. Y. Hughes, D. P. Bowman, R. Daniels, and T. Boden, 1996: *United States Historical Climatology Network (US HCN), Monthly Temperature and Precipitation Data*. Oak Ridge National Laboratory, Environmental Sciences Division, Carbon Dioxide Information Analysis Center,.

596 Elsner, M. M., S. Gangopadhyay, T. Pruitt, L. D. Brekke, N. Mizukami, and M. P. Clark, 2014: How
597 Does the Choice of Distributed Meteorological Data Affect Hydrologic Model Calibration and
598 Streamflow Simulations? *J. Hydrometeor*, **15**, 1384–1403, doi:10.1175/JHM-D-13-083.1.

599 Frei, A., K. E. Kunkel, and A. Matonse, 2015: The Seasonal Nature of Extreme Hydrological Events in
600 the Northeastern United States. *J. Hydrometeor*, **16**, 2065–2085, doi:10.1175/JHM-D-14-0237.1.

601 Frei, C., and C. Schär, 2001: Detection Probability of Trends in Rare Events: Theory and Application to
602 Heavy Precipitation in the Alpine Region. *J. Climate*, **14**, 1568–1584, doi:10.1175/1520-
603 0442(2001)014<1568:DPOTIR>2.0.CO;2.

604 Groisman, P. Y., R. W. Knight, T. R. Karl, D. R. Easterling, B. Sun, and J. H. Lawrimore, 2004:
605 Contemporary Changes of the Hydrological Cycle over the Contiguous United States: Trends
606 Derived from In Situ Observations. *J. Hydrometeor*, **5**, 64–85, doi:10.1175/1525-
607 7541(2004)005<0064:CCOTHC>2.0.CO;2.

608 Hayhoe, K., and Coauthors, 2004: Emissions pathways, climate change, and impacts on California.
609 *Proceedings of the National Academy of Sciences of the United States of America*, **101**, 12422–
610 12427, doi:10.1073/pnas.0404500101.

611 —, and Coauthors, 2007: Past and future changes in climate and hydrological indicators in the US
612 Northeast. *Clim Dyn*, **28**, 381–407, doi:10.1007/s00382-006-0187-8.

613 Higgins, R. W., V. B. S. Silva, W. Shi, and J. Larson, 2007: Relationships between Climate Variability
614 and Fluctuations in Daily Precipitation over the United States. *J. Climate*, **20**, 3561–3579,
615 doi:10.1175/JCLI4196.1.

616 Hoerling, M., J. Eischeid, J. Perlwitz, X.-W. Quan, K. Wolter, and L. Cheng, 2016: Characterizing Recent
617 Trends in U.S. Heavy Precipitation. *J. Climate*, **29**, 2313–2332, doi:10.1175/JCLI-D-15-0441.1.

618 Killick, R., P. Fearnhead, and I. A. Eckley, 2012: Optimal Detection of Changepoints With a Linear
619 Computational Cost. *Journal of the American Statistical Association*, **107**, 1590–1598,
620 doi:10.1080/01621459.2012.737745.

621 Kunkel, K. E., D. R. Easterling, D. A. R. Kristovich, B. Gleason, L. Stoecker, and R. Smith, 2010: Recent
622 increases in U.S. heavy precipitation associated with tropical cyclones. *Geophysical Research*
623 *Letters*, **37**, n/a – n/a, doi:10.1029/2010GL045164.

624 —, —, D. A. R. Kristovich, B. Gleason, L. Stoecker, and R. Smith, 2012: Meteorological Causes of
625 the Secular Variations in Observed Extreme Precipitation Events for the Conterminous United
626 States. *J. Hydrometeor*, **13**, 1131–1141, doi:10.1175/JHM-D-11-0108.1.

627 —, and Coauthors, 2013a: Monitoring and Understanding Trends in Extreme Storms: State of
628 Knowledge. *Bull. Amer. Meteor. Soc.*, **94**, 499–514, doi:10.1175/BAMS-D-11-00262.1.

629 Kunkel, K. E., and Coauthors, 2013b: *Regional Climate Trends and Scenarios for the U.S. National*
630 *Climate Assessment: Part 1. Climate of the Northeast*. US Department of Commerce, National
631 Oceanic and Atmospheric Administration, National Environmental Satellite, Data, and
632 Information Service,
633 [http://www.nesdis.noaa.gov/technical_reports/NOAA_NESDIS_Tech_Report_142-1-](http://www.nesdis.noaa.gov/technical_reports/NOAA_NESDIS_Tech_Report_142-1-Climate_of_the_Northeast_U.S.pdf)
634 [Climate_of_the_Northeast_U.S.pdf](http://www.nesdis.noaa.gov/technical_reports/NOAA_NESDIS_Tech_Report_142-1-Climate_of_the_Northeast_U.S.pdf).

635 Legates, D. R., and T. L. DeLiberty, 1993: PRECIPITATION MEASUREMENT BIASES IN THE
636 UNITED STATES1. *JAWRA Journal of the American Water Resources Association*, **29**, 855–
637 861, doi:10.1111/j.1752-1688.1993.tb03245.x.

638 Livneh, B., E. A. Rosenberg, C. Lin, B. Nijssen, V. Mishra, K. M. Andreadis, E. P. Maurer, and D. P.
639 Lettenmaier, 2013: A Long-Term Hydrologically Based Dataset of Land Surface Fluxes and
640 States for the Conterminous United States: Update and Extensions*. *Journal of Climate*, **26**,
641 9384–9392, doi:10.1175/JCLI-D-12-00508.1.

642 —, T. J. Bohn, D. W. Pierce, F. Munoz-Arriola, B. Nijssen, R. Vose, D. R. Cayan, and L. Brekke,
643 2015: A spatially comprehensive, hydrometeorological data set for Mexico, the U.S., and
644 Southern Canada 1950–2013. *Scientific Data*, **2**, 150042.

645 Luo, Y., E. H. Berbery, K. E. Mitchell, and A. K. Betts, 2007: Relationships between Land Surface and
646 Near-Surface Atmospheric Variables in the NCEP North American Regional Reanalysis. *J.*
647 *Hydrometeor*, **8**, 1184–1203, doi:10.1175/2007JHM844.1.

648 Marquardt Collow, A. B., M. G. Bosilovich, and R. D. Koster, 2016: Large-Scale Influences on
649 Summertime Extreme Precipitation in the Northeastern United States. *J. Hydrometeor.*, **17**, 3045–
650 3061, doi:10.1175/JHM-D-16-0091.1.

651 Maurer, E. P., A. W. Wood, J. C. Adam, D. P. Lettenmaier, and B. Nijssen, 2002: A Long-Term
652 Hydrologically Based Dataset of Land Surface Fluxes and States for the Conterminous United
653 States*. *Journal of Climate*, **15**, 3237–3251.

654 Menne, M. J., and Coauthors, 2012a: Global Historical Climatology Network-Daily (GHCN-Daily),
655 Version 3.21. *NOAA National Climatic Data Center*,. <http://doi.org/10.7289/V5D21VHZ>
656 (Accessed June 15, 2015).

657 Menne, M. J., I. Durre, R. S. Vose, B. E. Gleason, and T. G. Houston, 2012b: An Overview of the Global
658 Historical Climatology Network-Daily Database. *J. Atmos. Oceanic Technol.*, **29**, 897–910,
659 doi:10.1175/JTECH-D-11-00103.1.

660 Mesinger, F., and Coauthors, 2006: North American Regional Reanalysis. *Bull. Amer. Meteor. Soc.*, **87**,
661 343–360, doi:10.1175/BAMS-87-3-343.

662 Milrad, S. M., E. H. Atallah, and J. R. Gyakum, 2012: Precipitation Modulation by the Saint Lawrence
663 River Valley in Association with Transitioning Tropical Cyclones. *Wea. Forecasting*, **28**, 331–
664 352, doi:10.1175/WAF-D-12-00071.1.

665 Mishra, V., J. M. Wallace, and D. P. Lettenmaier, 2012: Relationship between hourly extreme
666 precipitation and local air temperature in the United States. *Geophysical Research Letters*, **39**, n/a
667 – n/a, doi:10.1029/2012GL052790.

668 Mo, K. C., M. Chelliah, M. L. Carrera, R. W. Higgins, and W. Ebisuzaki, 2005: Atmospheric Moisture
669 Transport over the United States and Mexico as Evaluated in the NCEP Regional Reanalysis. *J.*
670 *Hydrometeor*, **6**, 710–728, doi:10.1175/JHM452.1.

671 Peterson, T. C., and Coauthors, 2013: Monitoring and Understanding Changes in Heat Waves, Cold
672 Waves, Floods, and Droughts in the United States: State of Knowledge. *Bull. Amer. Meteor. Soc.*,
673 **94**, 821–834, doi:10.1175/BAMS-D-12-00066.1.

- Prein, A. F., R. M. Rasmussen, K. Ikeda, C. Liu, M. P. Clark, and G. J. Holland, 2017: The future intensification of hourly precipitation extremes. *Nature Clim. Change*, **7**, 48–52.
- Trenberth, K., 1998: Atmospheric Moisture Residence Times and Cycling: Implications for Rainfall Rates and Climate Change. *Climatic Change*, **39**, 667–694, doi:10.1023/A:1005319109110.
- Vose, R. S., and Coauthors, 2014: Improved Historical Temperature and Precipitation Time Series for U.S. Climate Divisions. *J. Appl. Meteor. Climatol.*, **53**, 1232–1251, doi:10.1175/JAMC-D-13-0248.1.
- Walsh, J., and Coauthors, 2014: Ch. 2: Our Changing Climate. *Climate Change Impacts in the United States: The Third National Climate Assessment*, J.M. Melillo, T.C. Richmond, and G.W. Yohe, Eds., U.S. Global Change Research Program, p. 841.
- Westerling, A. L., H. G. Hidalgo, D. R. Cayan, and T. W. Swetnam, 2006: Warming and Earlier Spring Increase Western U.S. Forest Wildfire Activity. *Science*, **313**, 940–943, doi:10.1126/science.1128834.
- Wood, A. W., L. R. Leung, V. Sridhar, and D. P. Lettenmaier, 2004: Hydrologic implications of dynamical and statistical approaches to downscaling climate model outputs. *Climatic Change*, **62**, 189–216.
- Wu, H., M. J. Hayes, D. A. Wilhite, and M. D. Svoboda, 2005: The effect of the length of record on the standardized precipitation index calculation. *International Journal of Climatology*, **25**, 505–520, doi:10.1002/joc.1142.
- Xie, P., M. Chen, S. Yang, A. Yatagai, T. Hayasaka, Y. Fukushima, and C. Liu, 2007: A Gauge-Based Analysis of Daily Precipitation over East Asia. *J. Hydrometeorol.*, **8**, 607–626, doi:10.1175/JHM583.1.

Tables

Table 1: Means and trends of GHCN-D annual total precipitation. The trends are calculated from simple linear regression. The symbols, * and #, denote the trend is significant at 0.05 level using parametric method (t-test) and nonparametric method (Mann-Kendall test), respectively. Percentage trends are calculated by dividing the linearly modeled change per decade by the value of the start year.

	Units	1901–2014	1915–2011	1979–2014	1979–2011
Mean	mm yr ⁻¹	1063	1059	1104	1104
Trend	mm decade ⁻¹	6.0*	11.1*	40.8*#	52.8*#
Trend	% decade ⁻¹	0.6	1.1	4.0	5.2

Table 2: Means and trends of annual extreme precipitation in GHCN-D dataset. The trends are calculated from Theil-Sen robust linear regression. A # denotes the trend is significant at 0.05 level using Mann-Kendall test. Percentage trends are calculated by dividing the linearly modeled change per decade by the value of the start year.

	Units	1901–2014	1915–2011	1979–2014	1979–2011
Mean	mm yr ⁻¹	82.4	83.0	97.4	97.3
Trend	mm decade ⁻¹	2.4 [#]	3.1 [#]	13.9 [#]	19.7 [#]
Trend	% decade ⁻¹	3.6	4.6	19.2	30.3

Table 3: Means and trends of GHCN-D seasonal total precipitation. The trends are calculated from simple linear regression. The symbols, * and #, denote the trend is significant at 0.05 level using parametric method (t-test) and nonparametric method (Mann-Kendall test), respectively. Percentage trends are calculated by dividing the linearly modeled change per decade by the value of the start year.

	Units	1901–2014	1915–2011	1979–2014	1979–2011
Spring					
Mean	mm yr ⁻¹	267.3	265.7	278.1	279.6
Trend	mm decade ⁻¹	0.9	3.0	4.4	8.6
Trend	% decade ⁻¹	0.4	1.2	1.6	3.2
Summer					
Mean	mm yr ⁻¹	302.4	299.7	313.0	309.4
Trend	mm decade ⁻¹	0.9	1.6	18.3 ^{*#}	16.6
Trend	% decade ⁻¹	0.3	0.5	6.5	5.9
Fall					
Mean	mm yr ⁻¹	262.3	265.4	285.2	287.9
Trend	mm decade ⁻¹	4.8 ^{*#}	6.0 ^{*#}	6.8	14.5
Trend	% decade ⁻¹	2.1	2.5	2.5	5.5
Winter					
Mean	mm yr ⁻¹	233.9	229.0	226.0	225.0
Trend	mm decade ⁻¹	-1.8	0.6	18.1 ^{*#}	21.8 ^{*#}
Trend	% decade ⁻¹	-0.7	0.3	9.3	11.5

Table 4: Means and trends of GHCN-D seasonal extreme precipitation. The trends are calculated from Theil-Sen robust linear regression. A # denotes the trend is significant at 0.05 level using Mann-Kendall test. Percentage trends are calculated by dividing the linearly modeled change per decade by the value of the start year.

Units	1901–2014	1915–2011	1979–2014	1979–2011
-------	-----------	-----------	-----------	-----------

Spring					
Mean	mm yr ⁻¹	18.1	17.7	25.1	24.6
Trend	mm decade ⁻¹	0.8 [#]	1.2 [#]	4.1	4.4
Trend	% decade ⁻¹	6.4	10.2	23.2	25.0
Summer					
Mean	mm yr ⁻¹	22.9	23.0	25.0	24.8
Trend	mm decade ⁻¹	0.2	0.1	2.5	2.4
Trend	% decade ⁻¹	0.9	0.6	12.4	11.8
Fall					
Mean	mm yr ⁻¹	21	21.8	26.7	27.1
Trend	mm decade ⁻¹	0.6	0.8	3.5	5.3
Trend	% decade ⁻¹	3.4	4.8	17.1	28.8
Winter					
Mean	mm yr ⁻¹	15.1	15.0	17.3	17.4
Trend	mm decade ⁻¹	0.5 [#]	0.9 [#]	3.8 [#]	5.3 [#]
Trend	% decade ⁻¹	4.3	8.3	35.3	57.5

Table 5: Means and trends of GHCN-D, LI2013, and NARR annual total precipitation. An x denotes a combination of time period and dataset that is not available. The trends are calculated from simple linear regression. The symbols, * and #, denote the trend is significant at 0.05 level using parametric method (t-test) and nonparametric method (Mann-Kendall test), respectively.

	Units	1901–2014	1915–2011	1979–2014	1979–2011
Mean					
GHCN-D	mm yr ⁻¹	1063	1071	1111	1110
LI2013	mm yr ⁻¹	x	1088	x	1143
NARR	mm yr ⁻¹	x	x	1041	1052
Trend					
GHCN-D	mm decade ⁻¹	6.0*	10.7*	46.4* [#]	56.8* [#]
LI2013	mm decade ⁻¹	x	12.4* [#]	x	54.2* [#]
NARR	mm decade ⁻¹	x	x	5.4	25.9

Table 6: Means and trends of GHCN-D, LI2013, and NARR annual extreme precipitation. An x denotes a combination of time period and dataset that is not available. The trends are calculated from Theil-Sen robust linear regression. A # denotes the trend is significant at 0.05 level using Mann-Kendall test.

	Units	1901–2014	1915–2011	1979–2014	1979–2011
Mean					
GHCN-D	mm yr ⁻¹	82.4	82.3	86.0	85.6
LI2013	mm yr ⁻¹	x	83.9	x	85.1
NARR	mm yr ⁻¹	x	x	77.5	77.9
Trend					
GHCN-D	mm decade ⁻¹	2.4 [#]	2.3 [#]	12.6 [#]	14.7 [#]
LI2013	mm decade ⁻¹	x	1.3	x	12
NARR	mm decade ⁻¹	x	x	4.9	15.8 [#]

Table 7: Means and trends of GHCN-D, LI2013, and NARR seasonal total precipitation. An x denotes a combination of time period and dataset that is not available. The trends are calculated from simple linear regression. The symbols, * and #, denote the trend is significant at 0.05 level using parametric method (t-test) and nonparametric method (Mann-Kendall test), respectively.

	Units	1901–2014	1915–2011	1979–2014	1979–2011
Spring Mean					
GHCN-D	mm yr ⁻¹	267.3	262.7	282.4	283.6
LI2013	mm yr ⁻¹	x	273	x	290.5
NARR	mm yr ⁻¹	x	x	272.8	277.3
Spring Trend					
GHCN-D	mm decade ⁻¹	0.9	2.6	7.0	11.1
LI2013	mm decade ⁻¹	x	3.6*	x	9.2
NARR	mm decade ⁻¹	x	x	4.1	-2.8
Summer Mean					
GHCN-D	mm yr ⁻¹	302.4	299.6	309.8	307.1
LI2013	mm yr ⁻¹	x	302.5	x	315
NARR	mm yr ⁻¹	x	x	279.5	281.2
Summer Trend					
GHCN-D	mm decade ⁻¹	0.9	1.8	17.0*#	16.3
LI2013	mm decade ⁻¹	x	2.1	x	16
NARR	mm decade ⁻¹	x	x	2.9	7.4
Fall Mean					
GHCN-D	mm yr ⁻¹	262.3	268.3	285.2	286.9
LI2013	mm yr ⁻¹	x	272.6	x	296.8
NARR	mm yr ⁻¹	x	x	261.5	265.2
Fall Trend					
GHCN-D	mm decade ⁻¹	4.8*#	5.9*#	9.9	16.4
LI2013	mm decade ⁻¹	x	5.9*#	x	15.5
NARR	mm decade ⁻¹	x	x	-1	5.7
Winter Mean					
GHCN-D	mm yr ⁻¹	233.9	228.6	231.5	230.1
LI2013	mm yr ⁻¹	x	239.2	x	236.5
NARR	mm yr ⁻¹	x	x	223.4	223.1
Winter Trend					

GHCN-D	mm decade ⁻¹	-1.8	0.1	17.7* [#]	20.1* [#]
LI2013	mm decade ⁻¹	x	1.2	x	20.3* [#]
NARR	mm decade ⁻¹	x	x	11.5	15.9* [#]

Table 8: Means and trends of GHCN-D, LI2013, and NARR seasonal extreme precipitation. An x denotes a combination of time period and dataset that is not available. The trends are calculated from Theil-Sen robust linear regression. A # denotes the trend is significant at 0.05 level using Mann-Kendall test.

	Units	1901–2014	1915–2011	1979–2014	1979–2011
Spring Mean					
GHCN-D	mm yr ⁻¹	18.1	17.1	19.2	19.0
LI2013	mm yr ⁻¹	x	18.7	x	19.1
NARR	mm yr ⁻¹	x	x	18.4	18.6
Spring Trend					
GHCN-D	mm decade ⁻¹	0.9 [#]	0.8 [#]	3.8 [#]	3.7 [#]
LI2013	mm decade ⁻¹	x	0.6	x	2.5
NARR	mm decade ⁻¹	x	x	2.6	4.7 [#]
Summer Mean					
GHCN-D	mm yr ⁻¹	22.9	22.5	23.3	23.0
LI2013	mm yr ⁻¹	x	23.5	x	22.9
NARR	mm yr ⁻¹	x	x	19.7	19.6
Summer Trend					
GHCN-D	mm decade ⁻¹	0.2	0.2	2.9 [#]	2.8
LI2013	mm decade ⁻¹	x	-0.1	x	1.8
NARR	mm decade ⁻¹	x	x	2.2	2.7
Fall Mean					
GHCN-D	mm yr ⁻¹	21	21.6	22.7	22.7
LI2013	mm yr ⁻¹	x	22.2	x	22.9
NARR	mm yr ⁻¹	x	x	20.0	20.2
Fall Trend					
GHCN-D	mm decade ⁻¹	0.6	0.6	3.3	4.8
LI2013	mm decade ⁻¹	x	0.2	x	4.8
NARR	mm decade ⁻¹	x	x	1.7	5.0
Winter Mean					
GHCN-D	mm yr ⁻¹	15.1	15.1	16.1	16.1
LI2013	mm yr ⁻¹	x	16.7	x	16.1
NARR	mm yr ⁻¹	x	x	16.0	16.0
Winter Trend					
GHCN-D	mm decade ⁻¹	0.5 [#]	0.8 [#]	3.2	4.4 [#]
LI2013	mm decade ⁻¹	x	0.3	x	4.0 [#]
NARR	mm decade ⁻¹	x	x	2.4	4.4 [#]

Figure Caption List

- Figure 1: Time series of spatially averaged Northeast GHCN-D annual total precipitation from 1901–2014 with (a) nine trendlines for time periods starting in 1901, 1911, 1921, 1931, 1941, 1951, 1961, 1971, and 1981, and ending in 2014; and (b) dashed line denoting 1901–2014 average annual total precipitation and trendlines before and after the changepoint year of 2002. 35
- Figure 2: GHCN-D annual total precipitation (a) means 1901–2014, (b) trends 1901–2014, (c) trends 1915–2011, and (d) trends 1979–2014. In (b)–(d), square points represent significant trends while diamond points represent insignificant trends. 36
- Figure 3: Time series of spatially averaged Northeast GHCN-D annual extreme precipitation from 1901–2014 with (a) nine trendlines for time periods starting in 1901, 1911, 1921, 1931, 1941, 1951, 1961, 1971, and 1981, and ending in 2014; and (b) dashed line denoting 1901–2014 average annual extreme precipitation and trendlines before and after the changepoint year of 1996. 37
- Figure 4: GHCN-D annual extreme precipitation (a) means 1901–2014, (b) trends 1901–2014, (c) trends 1915–2011, and (d) trends 1979–2014. In (b)–(d), square points represent significant trends, diamond points represent insignificant trends, and white points represent undetectable trends or trends with zero slope. 38
- Figure 5: Percentage change in annual extreme precipitation between the periods 1996–2014 and 1901–1995 relative to 1901–1995. 39
- Figure 6: LI2013 (shading) and GHCN-D (points) annual total precipitation (a) means and (b) trends 1915–2011. NARR (shading) and GHCN-D (points) annual total precipitation (c) means and (d) trends 1979–2014. In (b) and (d), square points represent significant trends while diamond points represent insignificant trends. 40
- Figure 7: LI2013 (shading) and GHCN-D (points) annual extreme precipitation (a) means and (b) trends 1915–2011. NARR (shading) and GHCN-D (points) annual extreme precipitation (c) means and (d) trends 1979–2014. In (b) and (d), square points represent significant trends, diamond points represent insignificant trends, and white points represent undetectable trends or trends with zero slope. 41

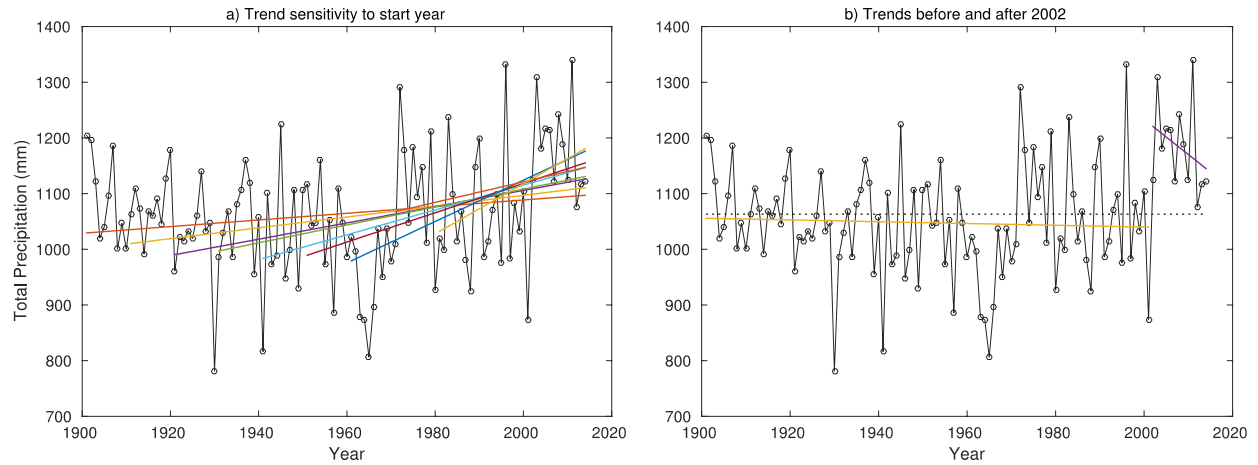


Figure 1: Time series of spatially averaged Northeast GHCN-D annual total precipitation from 1901–2014 with (a) nine trendlines for time periods starting in 1901, 1911, 1921, 1931, 1941, 1951, 1961, 1971, and 1981, and ending in 2014; and (b) dashed line denoting 1901–2014 average annual total precipitation and trendlines before and after the changepoint year of 2002.

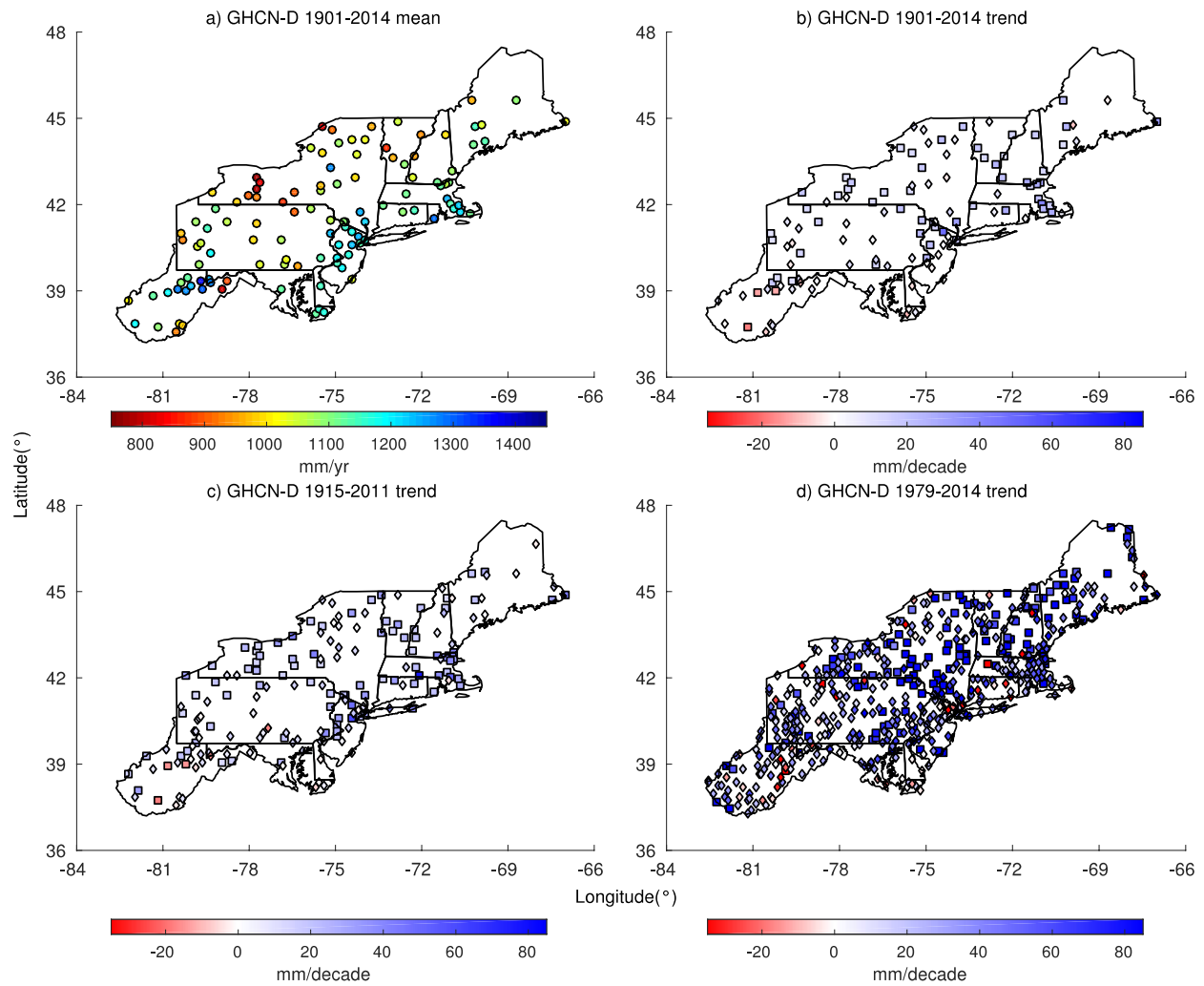


Figure 2: GHCN-D annual total precipitation (a) means 1901–2014, (b) trends 1901–2014, (c) trends 1915–2011, and (d) trends 1979–2014. In (b)–(d), square points represent significant trends while diamond points represent insignificant trends.

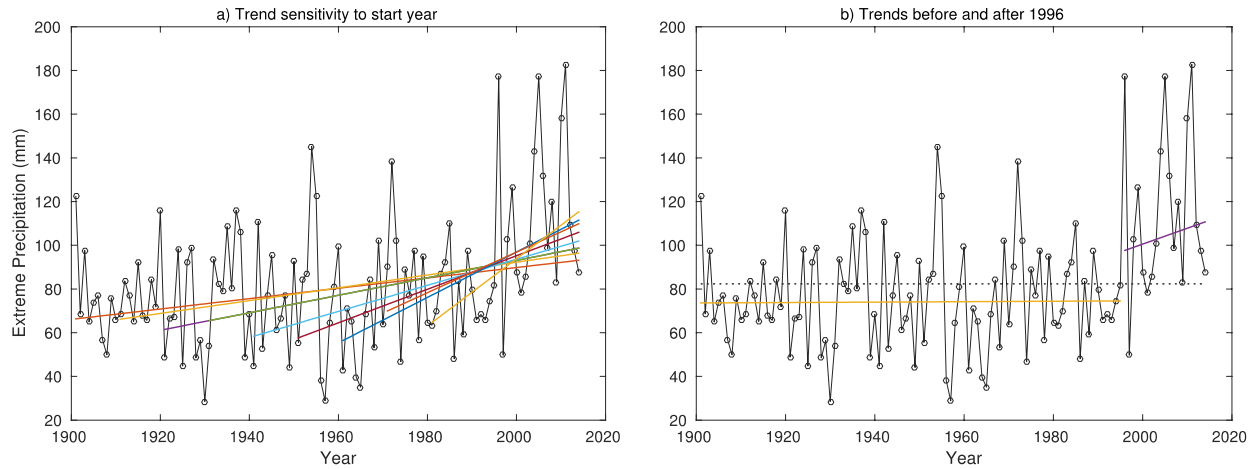


Figure 3: Time series of spatially averaged Northeast GHCN-D annual extreme precipitation from 1901–2014 with (a) nine trendlines for time periods starting in 1901, 1911, 1921, 1931, 1941, 1951, 1961, 1971, and 1981, and ending in 2014; and (b) dashed line denoting 1901–2014 average annual extreme precipitation and trendlines before and after the changepoint year of 1996.

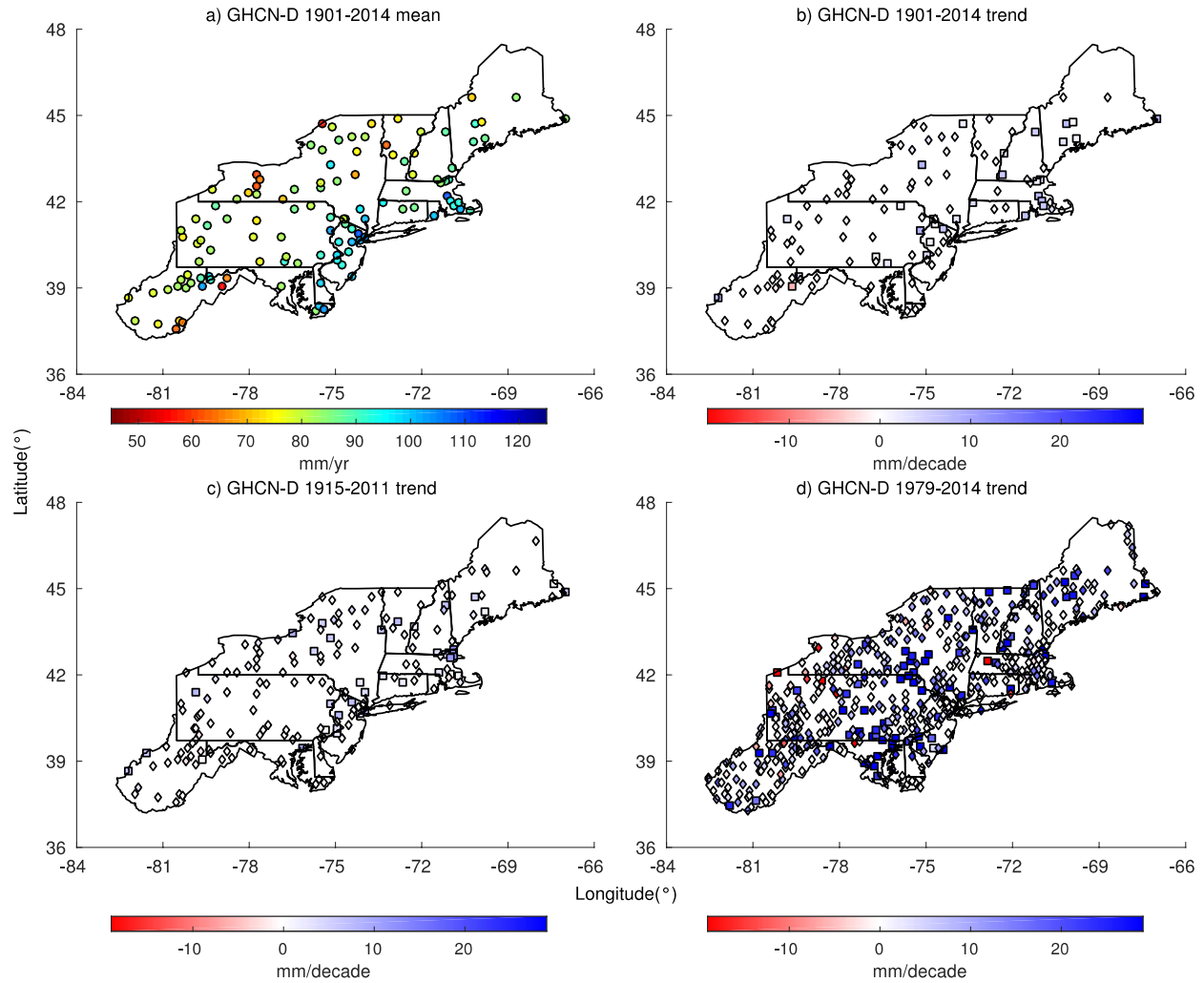


Figure 4: GHCN-D annual extreme precipitation (a) means 1901–2014, (b) trends 1901–2014, (c) trends 1915–2011, and (d) trends 1979–2014. In (b)–(d), square points represent significant trends, diamond points represent insignificant trends, and white points represent undetectable trends or trends with zero slope.

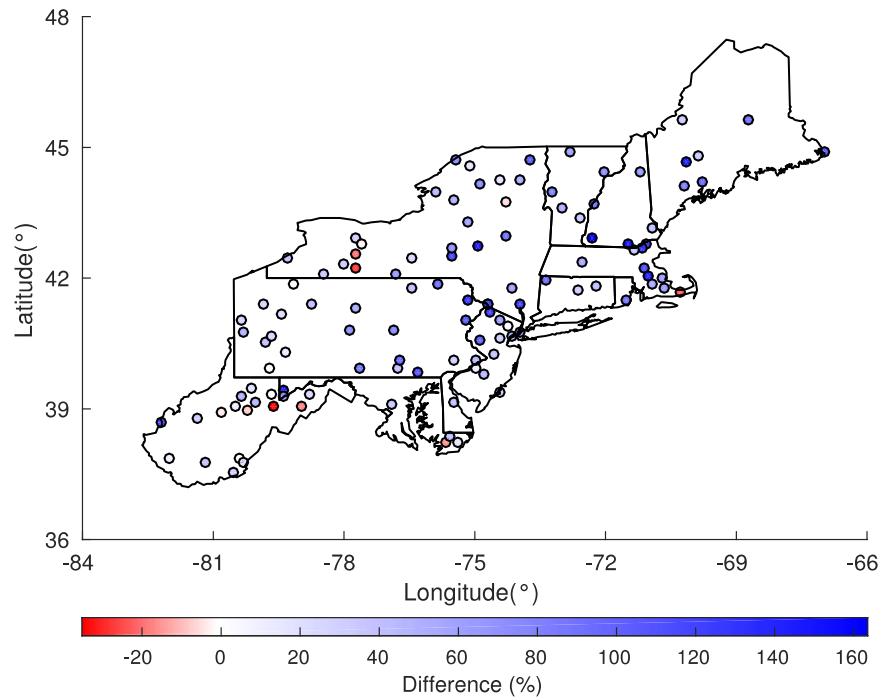


Figure 5: Percentage change in annual extreme precipitation between the periods 1996–2014 and 1901–1995 relative to 1901–1995.

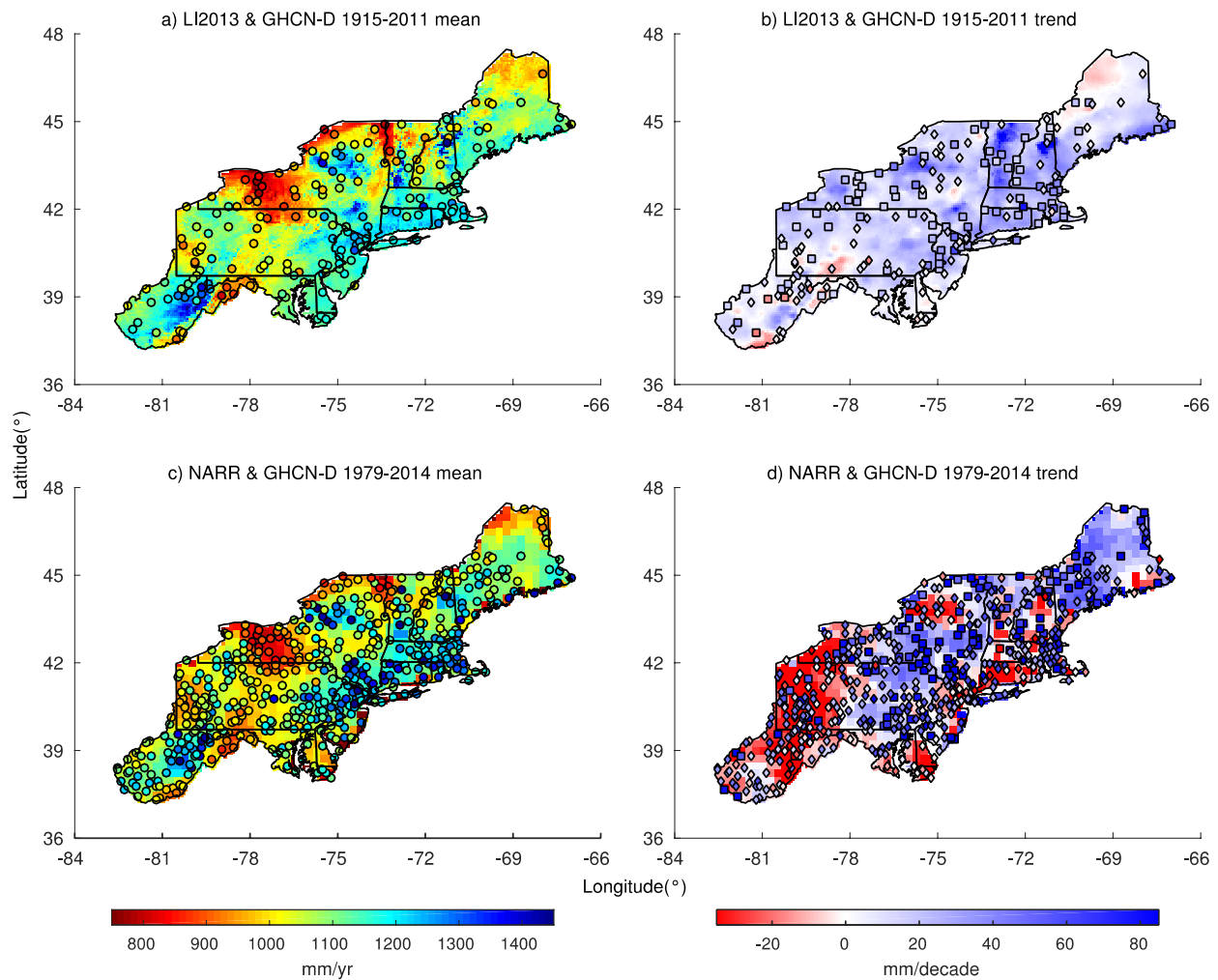


Figure 6: LI2013 (shading) and GHCN-D (points) annual total precipitation (a) means and (b) trends 1915–2011.

NARR (shading) and GHCN-D (points) annual total precipitation (c) means and (d) trends 1979–2014. In (b) and (d), square points represent significant trends while diamond points represent insignificant trends.

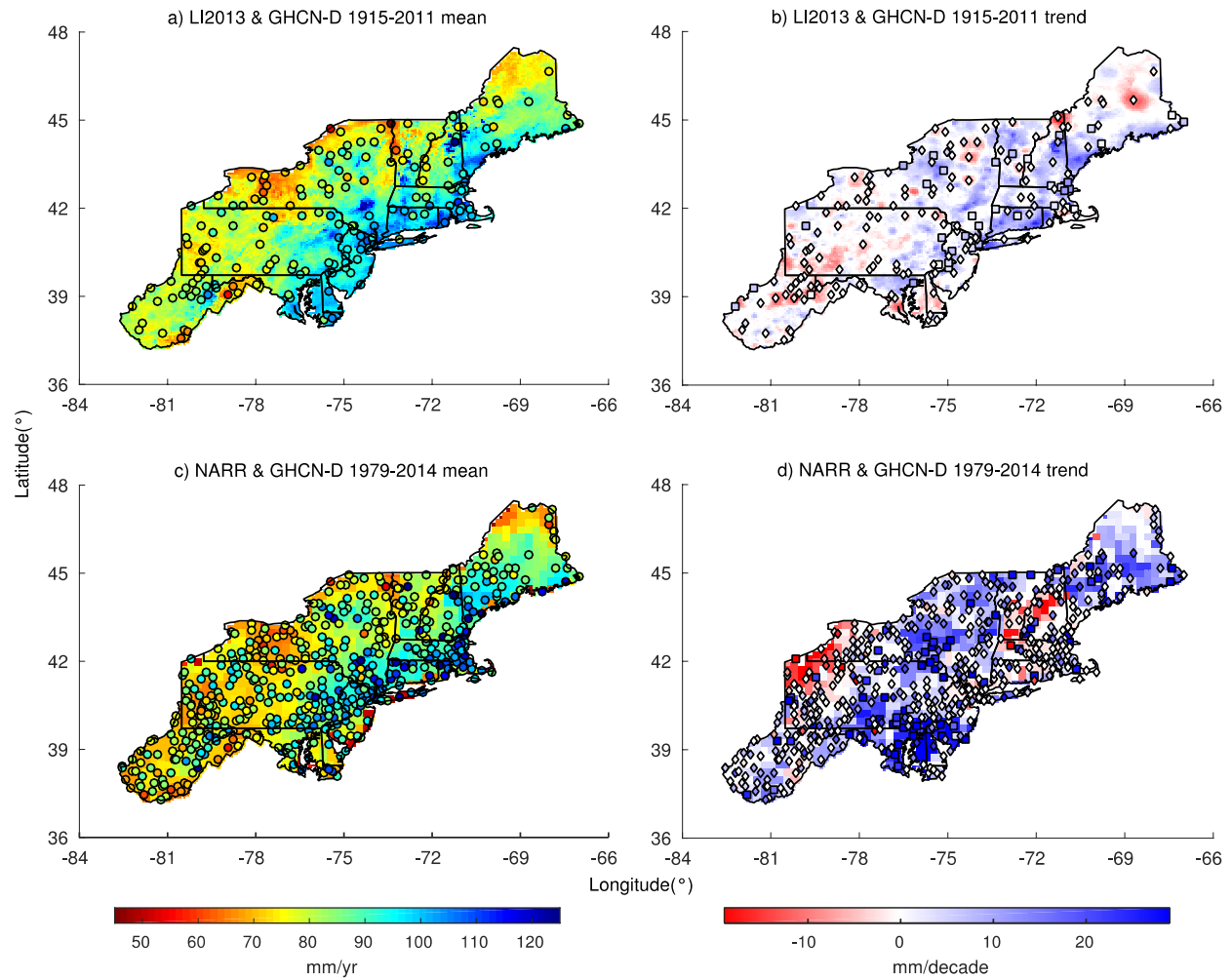


Figure 7: LI2013 (shading) and GHCN-D (points) annual extreme precipitation (a) means and (b) trends 1915–2011. NARR (shading) and GHCN-D (points) annual extreme precipitation (c) means and (d) trends 1979–2014. In (b) and (d), square points represent significant trends, diamond points represent insignificant trends, and white points represent undetectable trends or trends with zero slope.